Addendum to A Power Resolution for Nonsinusoidal and Unbalanced Systems: Evaluation Examples

M. E. Balci and M. H. Hocaoglu

Abstract—**In this paper, a power resolution presented in [1] is evaluated by considering optimum balanced capacitive compensation and harmonic producing load detection issues. The evaluation examples show that the power resolution can be employed to directly measure the optimum balanced capacitors bank's power and obtain some useful information on the harmonic source detection.**

Index Terms-- **Apparent power definitions, power resolutions, nonsinusoidal conditions, unbalanced systems, optimum balanced capacitive compensation, harmonic source detection.**

I. Background

The theoretical background of the proposed power resolution, which aims to directly determine the power of the optimum balanced capacitors bank and detect the harmonic producing loads, is presented in [1].

The evaluation examples of the power resolution are presented in this paper. First, in section II, it is evaluated for the optimum balanced capacitive compensation using simulation of a test case. Second, in section III, using the statistical results obtained from the experimental measurements it is also shown that the power resolution can give some useful information on the detection of the harmonic producing loads.

II. Exemplary Simulation for Optimum Balanced Capacitive Compensation

In this section, it is demonstrated that the proposed resolution can be used as a tool to obtain the power of optimum balanced capacitors bank. Hence, the unity power factor can be achieved cost effectively by the parallel combination of the optimum balanced capacitors bank and an active compensator (hybrid compensation). In other words, after the optimum balanced capacitive compensation, the magnitude of balanced power could be minimized. Therefore, the power of active compensator in the hybrid compensation scheme could be smaller than used in pure active compensation scheme. The merit of the proposed resolution for the direct implementation of hybrid compensation will be examined in a test case, given in [2].

For the system without compensation (NC), with optimum balanced capacitive compensation (PC), active compensation (AC) and hybrid compensation (HC), the calculated power components of proposed resolution (P, Q_r, D_{sc}, D_{ss}, D_{up} and D_{uq}), apparent power (S), the powers of passive and active compensators (S_{pC} and S_{aC}) and power factor (pf) are given in Fig. 1. It should be noted that active compensation is undertaken by unity power factor compensation strategy [3]. Fig. 1 shows that the power factor, reactive power and apparent power of the system without compensation (NC) are 0.828, 0.445 pu and 1.000 pu. In optimum balanced capacitive compensation (PC) case, the reactive power is completely compensated and power factor is improved from 0.828 to 0.926 by using a balanced capacitors bank, of which power is measured as 0.445 pu under the voltages of the test case. Obviously, apart from the reactive power, all power components remain the same as their values measured before the compensation. Thus, one can see that proposed reactive power gives the power of optimum balanced capacitors bank under the load terminal voltage. But, power factor is still smaller than unity for the case. For active compensation (AC) case, unity power factor is achieved by only active compensator, of which power is equal to 0.559 pu, and apparent power decreased to 0.828 pu. On the other hand, for hybrid compensation (HC) case, unity power factor is achieved by using the optimum balanced capacitors bank, of which power is measured as 0.445 pu under the voltages of the test system, and an active compensator, of which power is equal to 0.336 pu. The depicted results conclude that power factor can be unity by active and hybrid compensations. Moreover, the power of active compensator, used in hybrid compensation, is 60.1% of active compensator's power used in pure active compensation.

In addition to above mentioned results, conventional capacitive compensation method already implemented in the reactive power control relays selects the balanced capacitors bank of which power is equal to three times of the fundamental harmonic reactive power measured at any one of the phases [4]-[6]. According to the conventional method,

This work was supported by Turkish Scientific Research Council (TUBITAK) under the project number 111E113.

M. E. Balci is with Balikesir University, Balikesir, TURKEY (e-mail: mbalci@balikesir.edu.tr).

M. H. Hocaoglu is with Gebze Institute of Technology, Kocaeli, TURKEY (e-mail: hocaoglu@gyte.edu.tr).

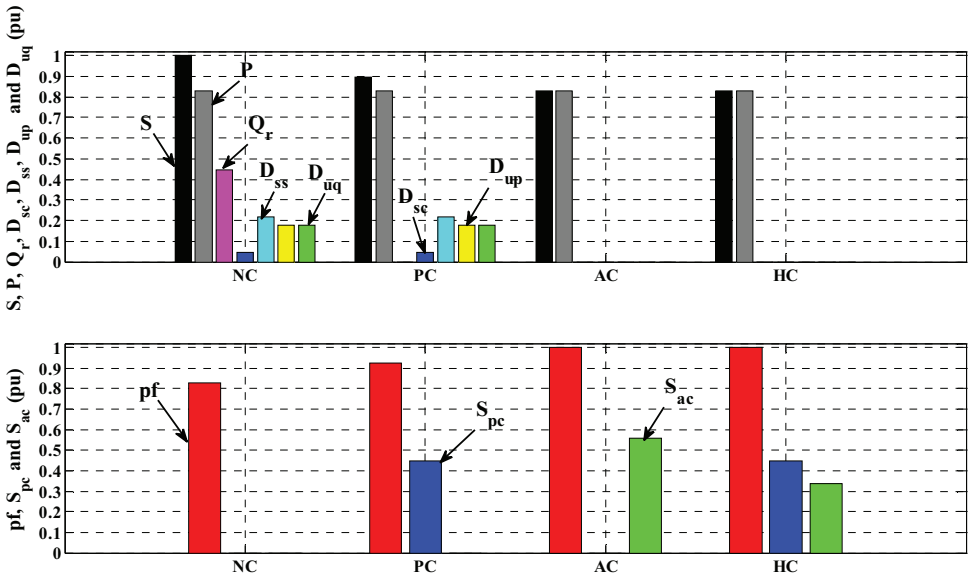

Fig. 1: The powers and power factors for the NC, PC, AC and HC cases.

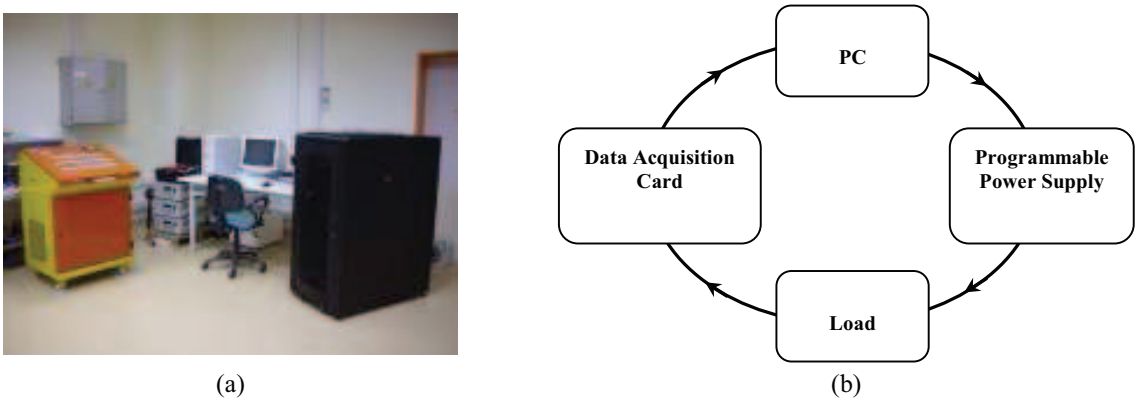

(a) (b)

Fig. 2: (a) The test system and (b) its schematic.

when the balanced capacitors bank, of which fundamental harmonic reactive power is equal to 0.702 pu (three times of the fundamental harmonic reactive power measured at phase a, 0.234 pu), is used for passive compensation, power factor is increased from 0.828 to 0.881. Furthermore, if this balanced capacitors bank and an active compensator are connected in parallel; the unity power factor is achieved by using the active compensator, of which power is 79.9% of active compensator's power used in pure active compensation.

As a result, one can see that the parallel combination of the optimum balanced capacitors bank, which can be determined by the proposed resolution, and an active compensator could be used for the unity power factor compensation with a cost effective manner.

III. Exemplary Measurements for Detection of Harmonic Producing Loads

The harmonic producing load detection method based on the proposed power resolution is statistically evaluated for some test voltages and load types here. The system used for the evaluation of proposed resolution on the detection of harmonic producing loads and its schematic are depicted in Fig. 2.

The test system, given in Fig. 2 (a), consists of a PC, a data acquisition card, a load and a programmable power supply. In the schematic, presented in Fig. 2 (b), PC processes voltage and current data, and controls the programmable power supply. R-L impedance with R/Z=0.89, a number of computers and a number of compact fluorescent lamps are the load types used in the test system. Each one of these single-phase loads is supplied with one sinusoidal and one hundred different distorted voltages with 5 % value of THD_V, which are randomly produced by the programmable power supply. For the sinusoidal excitation, voltage and current pairs of these loads are plotted in Fig. 3.

It is shown from Fig. 3 (a) that the current of a R-L impedance under sinusoidal supply voltage is sinusoidal. For sinusoidal excitation, the distorted currents of the computers and compact fluorescent lamps, of which THD_I are measured

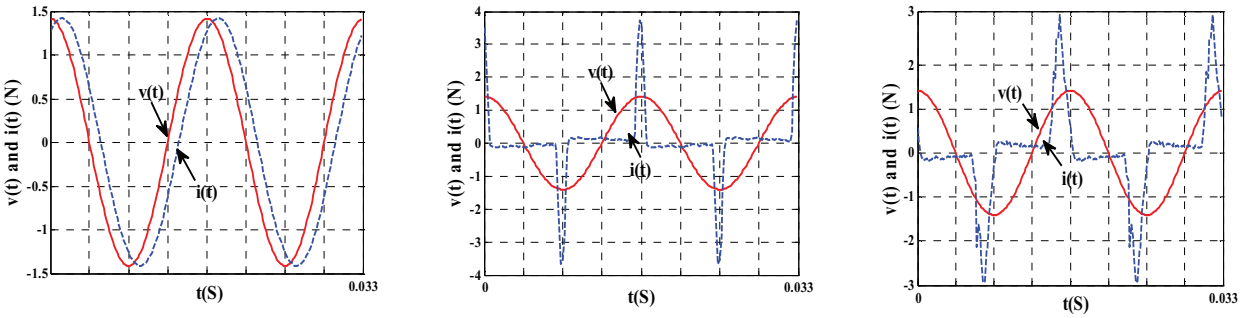

Fig. 3: For sinusoidal excitation, the voltage and current pairs of (a) the R-L impedance, (b) a number of computers and (c) a number of compact fluorescant lamps.

as 185% and 115%, respectively, are seen from Fig. 3 (b) and (c). For these loads, the normalised values of the proposed power components measured under sinusoidal supply voltage and the histograms of the normalised power components measured under distorted test voltages are presented in Fig. 4.

Fig. 4 (a) shows that the R-L impedance draws active (P) and reactive (Q_r) powers measured as 0.89 and 0.44, respectively. In addition, for the R-L impedance load the scattered conductance (D_{sc}) and scattered susceptance (D_{ss}) powers are almost zero. Fig. 4 (d) also shows that P, Q_r and D_{sc} measured under the distorted test voltages are very close to the measured values under sinusoidal supply voltage. However, for the distorted test voltages, D_{ss} varies between 0.1 and 0.2.

It is observed from Fig. 4 (b) that the P, Q_r, D_{sc} and D_{ss} of the computers are 0.45, 0.11, 0.53 and 0.7 for sinusoidal supply voltage. For the computers the histogram of Q_r, plotted in Fig. 4 (e), shows that the values of Q_r measured under sinusoidal and the distorted test voltages are very close to each other. For the distorted test voltages, P, D_{sc} and D_{ss} vary in the intervals from 0.4 to 0.6, from 0.5 to 0.9 and from 0.1 to 0.7, respectively.

It is seen from Fig. 4 (c) that the P, Q_r, D_{sc} and D_{ss} of the compact fluorescent lamps are measured as 0.54, 0.37, 0.63 and 0.41 in sinusoidal supply voltage case. In addition to that, for the compact fluorescent lamps under the distorted test voltages, the histograms plotted in Fig. 4 (f) show that P is in the interval between 0.4 and 0.6, Q_r is in the interval between 0.3 and 0.4, D_{sc} is in the interval between 0.3 and 0.7, and D_{ss} is in the interval between 0.3 and 0.7.

From statistical results given above, it is observed that D_{sc} has two distinct cases for the tested loads:

- Its normalised values measured for R-L impedance is very close to zero.
- However, for the harmonic producing loads, it has large normalised values.

As a result, this property of the D_{sc} could be useful to detect the harmonic producing loads.

IV. Conclusion

In this paper, the simulation results figure out that the reactive power component of the proposed power resolution can be utilized for the direct provision of the optimum balanced capacitors bank in the nonsinusoidal single-phase systems and three-phase & three-line systems, which consist of balanced & nonsinusoidal voltages and unbalanced & nonsinusoidal currents.

In addition to that, the experimental measurement results encourage that the scattered conductance power component of the proposed resolution can be useful for the detection of the harmonic producing loads. For the employability of the proposed power resolution on the detection of the harmonic producing loads, more load types will be tested in the future works.

V. Reference

[1] M. E. Balci, M. H. Hocaoglu, ‘‘A Power Resolution for Nonsinusoidal and Unbalanced Systems- Part II: Theoretical Backgorund’’, ELECO 2011, Bursa, TURKEY, 2011.

[2] M. E. Balci and M. H. Hocaoglu, ‘‘A Power Resolution for Nonsinusoidal and Unbalanced Systems- Part I: Literature Overview and Motivation’’, ELECO 2011, Bursa, TURKEY, 2011.

[3] H. Akagi, E. H. Watanabe, M. Aredes, ‘‘Instantaneous Power Theory and Applications to Power Conditioning,’’ 1st Edition, IEEE Press, John Wiley & Sons, 2007.

[4] ABB, ‘‘Modbus-Power Factor Controller Installation and Operating Instructions Manual’’, accessible on February 1st, 2010 from the web site,www.abb.com/product/seitp329/63468e43c00a1ce4c1256ee60035a458.aspx.

[5] COMAR Condensatori Co., ‘‘P.F.C. Electronic Regulator BMR Series User Manuel’’, accessible on June 1st, 2011, from the web site http://www.comarcond.com/tedesco/download_d/MU%2003.14.mmm%20REV3%20_BMR%20ENG.pdf.

[6] BARON Co., ‘‘Janitza Power Factor Control Relay Features’’, accessible on June 1st, 2011, from the web site http://www.baronpower.com/janitza.html.

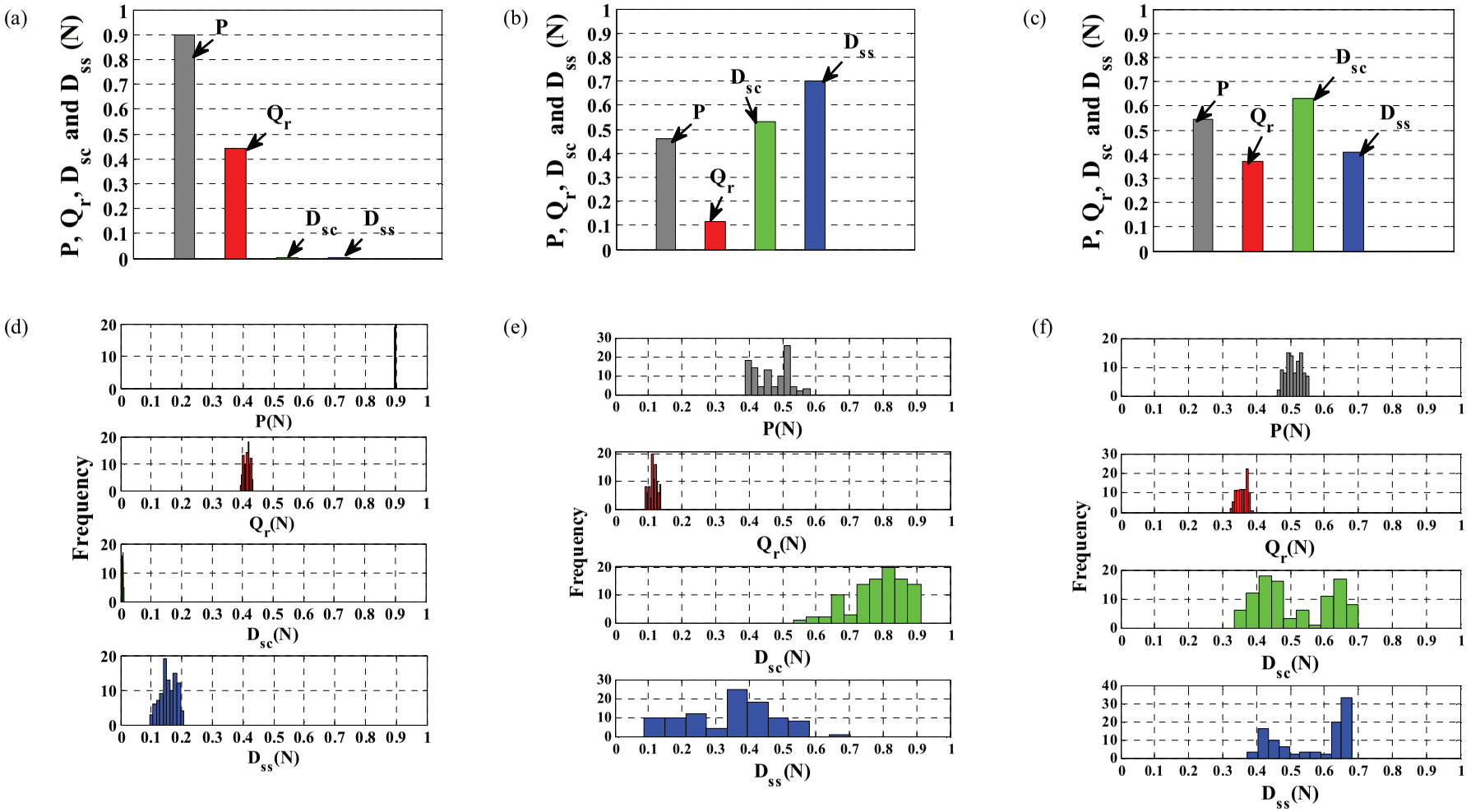

Fig. 4: The normalised values of P, Q_r, D_{sc} and D_{ss} measured under sinusoidal supply voltage for (a) a R-L impedance, (b) a number of computers and (c) a number of compact flourescant lamps, and the histograms of the normalised powers measured under distorted test voltages for (d) a R-L impedance, (e) a number of computers and (f) a number of compact flourescant lamps.